

Enhancement of Panel zone (PZ) contribution to the ductility of post-Northridge welded connections

AMIR A. HEDAYAT, MURUDE CELIKAG

Civil Engineering Department

Eastern Mediterranean University

P O Box. 95, Gazimagusa – North Cyprus, via Mersin 10

TURKEY

murude.celikag@emu.edu.tr

Abstract: In welded connections, beam-end and panel zone (PZ) are the only sources to dissipate the seismic energy released during an earthquake. Energy dissipation at the PZ is accompanied by the inelastic shear deformation at PZ. In seismic codes, in order to reach to the maximum plastic rotation capacity of connection, the inelastic shear deformation is controlled by a balance condition with respect to the initiation of flexural yielding of beam flanges. Hence, connections are classified as weak, balance and strong panel zone connections. In the case of weak PZ, balance condition can be obtained by increasing the thickness of the column's PZ or using doubler plates. This study was aimed to obtain balance condition for connections with strong panel zones. Therefore, a circular hole was opened at the column web in the PZ region. A pre-tested post-Northridge connection which has a strong panel zone was modeled using finite element analysis. Then the effects of different diameter holes on the behavior of this type of connection were investigated. Further, a function was proposed to determine the PZ shear yielding resistance in the presence of a circular hole in PZ. Analytical results showed that the column with a PZ hole ratio (hole diameter divided by PZ height) of 18% associated with a PZ hole of 50 mm radius and balance ratio of 0.81 appears to be the best configuration for increasing the PZ plastic rotation from 0.05% to 0.2%. This increase in plastic rotation capacity of PZ would only increase the total plastic rotation capacity of the connection by 10%. This indicates that a connection of this type also require modifications at the beam-end to increase both the total plastic rotation capacity and contribution of panel zone to the inelastic behavior of connection.

Key-Words: Post-Northridge connections; Panel zone; Ductility; Inelastic shear deformation

1 Introduction

Steel special moment-resisting frames (SMRF) are believed to have the capacity to develop the strength and ductility required to resist strong seismic loading. The released seismic energy is dissipated by forming plastic hinges in the steel frames. In steel connections, there are generally three sources to dissipate the seismic energies. These are panel zone (PZ), connecting elements to connect the beam-end to the column flanges and beam-end. The connecting elements include end-plate in extended end-plate bolted connections or angles in top-seat and two web angles connections. Among the three sources, connecting elements usually have the highest capacity to dissipate seismic energies [1]. In pre and post-Northridge welded connections, where the beam-end is directly welded to the column flanges, without any connecting element, the role of other two sources, PZ and beam-end, become very important.

Energy dissipation at the beam-end is accompanied by flexural yielding developed at the beam section near the column face. However, the panel zone dissipates seismic energies by developing the inelastic shear deformation when it yields.

In order to investigate the effect of PZ yielding on the behavior of welded connections, several experimental and analytical studies have been performed. The elastic and inelastic fracture analyzes of pre-Northridge and post-Northridge connections have shown that high shear stress in the panel zone and high stresses in the column flanges increase the fracture potential of the connection [2]. Therefore, fractures usually initiate at the CJP weld between the beam flange and column flange for pre-Northridge connections or around the weld access hole for post-Northridge connections. The brittle failure prevents the welded moment connections

from exhibiting the inelastic behavior required to resist earthquake loading and consequently reduces the capacity of the second energy dissipation source, beam-end. The most serious rupture modes of such connections [3] are shown in Fig. 1. Furthermore, the Crack Tip Opening Displacement (CTOD) ductility demand was higher in connections with higher panel zone yielding which implies that greater Charpy V-notch (CVN) toughness is required from the steel and weld metal if extensive panel zone yielding occurs [2].

The ABAQUS computer program was used to carry out a wide range of 3-dimensional nonlinear analyses of connections [4]. The potential for plastic yielding and fracture were evaluated at critical locations by using the Von-Mises and hydrostatic stress state parameters. These analyses showed that large panel zone deformations increase the hydrostatic and principle stresses at critical areas of the connection and increase the potential for connection fracture.

An experimental investigation was carried out on pre-Northridge connections, and on connections with the same geometry but with notch-tough weld filler metals [5]. The aim was to evaluate the effects of panel zone yielding and notch-tough filler metals. Some of the specimens were designed to have very strong panel zones while others had intermediate or very weak panel zones. The results did not provide a clear picture of the effect of panel zone yielding, since all specimens displayed minimal ductility. In some specimens, panel zone yielding caused a slight increase in ductility when compared to specimens with no panel zone yielding. Inelastic shear deformations were observed in specimens with weak panel zones, but, experiments indicate that they may have less plastic rotation capacity than those specimens with strong panel zones.

In addition, if the panel zone is very strong then no panel zone yielding occurs and the ductility may reduce. This means that the second source of dissipation of energy is eliminated [6]. Hence, a balance condition is defined in seismic codes as the achievement of both adequate plastic rotation and sufficient energy dissipation. This balance condition is achieved when shear yielding of the panel zone and flexural yielding of the beam occur at approximately the same load. If, however, the yielding of PZ starts before the yielding of the beam flanges then the connection is called a weak PZ connection. In the reverse case, it is known as a strong PZ connection.

In references [7] and [8] doubler plates were added to the column PZ to convert a weak PZ condition to a balance PZ condition. The results showed that an increase in PZ thickness can decrease the rupture index at the beam web welds; however, there is no reduction in rupture index at the root of the weld access hole (WAH) and at the complete joint penetration (CJP) weld between the beam flanges and the column flange.

So far, several attempts have been made to achieve a balance condition from weak PZ conditions, but no attempts have been made to achieve a balance condition from strong PZ conditions. This study aimed to achieve a balance condition from a strong PZ connection by opening circular holes in the column web at the PZ region. A pre-tested post-Northridge connection with a strong panel zone was modeled by using finite element analysis and its analytical results were compared to experimental results to verify the accuracy of modeling. Then, nine circular holes with different radiuses were considered at the column PZ and their effects on the behavior of the connection investigated. In addition, a function was proposed to determine the PZ shear yielding resistance in the presence of a circular hole at PZ. Finally, the most suitable circular hole radius was determined. The presence of this optimum radius helps to achieve the largest plastic rotation capacity of connection, and lowest PEEQ and rupture indexes at critical regions (CJP weld at intersection between beam flange and column flange, WAH root and CJP beam web welds).

2 Finite Element Modeling

Many factors are believed to contribute to the occurrence of brittle fracture at the weld joints, such as weld defects and notch effects, fracture toughness of deposited weld metal, high stress triaxiality due to severe structural restraint conditions and geometry of weld access holes. Therefore, the finite element method [9][10] was used to investigate the behavior of welded connections.

A pre-tested post-Northridge connection, specimen S6 of reference [11], was modeled using the general purpose finite element program ANSYS [12]. The size of members and the configuration of the weld access hole are shown in Fig.2. Fig.3 depicts the mesh of the finite element models of specimen S6 and the modified specimen with a typical circular hole opening in the PZ. The finite element model consisted of 15799 nodes and 9695 elements.

Solid element 45 was used to model the beam, column, shear tab, weld metal and bolts. The interaction between the surfaces of the shear tab and beam web, bolt head/nut and shear tab, and bolt shank and shear tab were modeled using node-to-node contact elements. For analyses, the Von-Mises yield criterion was used to account for material nonlinearity. Isotropic hardening was assumed for the analysis with monotonic loading, whereas kinematic hardening was assumed for the analysis with cyclic loading.

The stress-strain relations for steel plates and welds were simplified as a bilinear relationship with strain hardening, with a 4 percent modulus of elasticity. For the bolt materials, the three-linear relationship of reference [13] was used. The modulus of elasticity, yield stress and ultimate stress of bolts were selected as 217000 MPa [14], 893 MPa [15] and 974 MPa [15] respectively. The performed analysis included nonlinear geometric behavior where the effect of large deformations considered. The constraints applied to the model are in accordance with those applied to the test.

Since weakening of connection often causes the buckling of beam/column elements, Riks method was used to perform nonlinear analyses. In this method, first of all, using a separate buckling analysis, buckling mode shapes of a specimen were computed and then were used to perturb the original perfect geometry of the model. At the end, the imperfect model obtained was analyzed to consider the buckling behavior.

The analyses for monotonic behavior were conducted by applying a monotonic displacement load to the beam tip until a 3 percent plastic rotation was achieved. Meanwhile, the load history (Fig.4) was used for cyclic behavior. In load history, Δ_y represents the displacement at the end of cantilever when the beam has reached its yield moment.

In order to verify the accuracy of the modeling of specimen S6, the experimental and analytical results obtained from the finite element modeling were compared in terms of load and beam tip displacement. Fig.5 shows a good correlation between the analytical and experimental results.

3 Parametric Study

In FEMA [6], the balance condition is defined by ratio V_{PZ}^{My} / V_y , where V_{PZ}^{My} is the panel zone shear

force associated with the initiation of flexural yielding and V_y is the panel zone shear force when panel zone yielding occurs. The recommended interval for this ratio is 0.6 to 0.9 such that, those specimens with a ratio greater than 0.9 are weak and those with a ratio less than 0.6 are very strong. The best results are achieved when the ratio is close to 0.9.

For a panel zone without any holes, V_y can be calculated by using equation (1):

$$V_y = 0.55 \times F_{yc} \times d_c \times t_{wc} \quad (1)$$

This equation is based on the idea that yielding of PZ occurs when Von-Mises stress at PZ reaches the yield stress of PZ material. In this equation F_{yc} , d_c and t_{wc} are column web yield stress, column depth and panel zone thickness respectively.

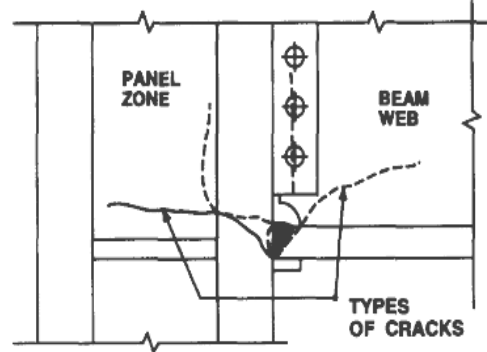


Fig. 1. Some failure modes of the welded beam-to-column connection [3]

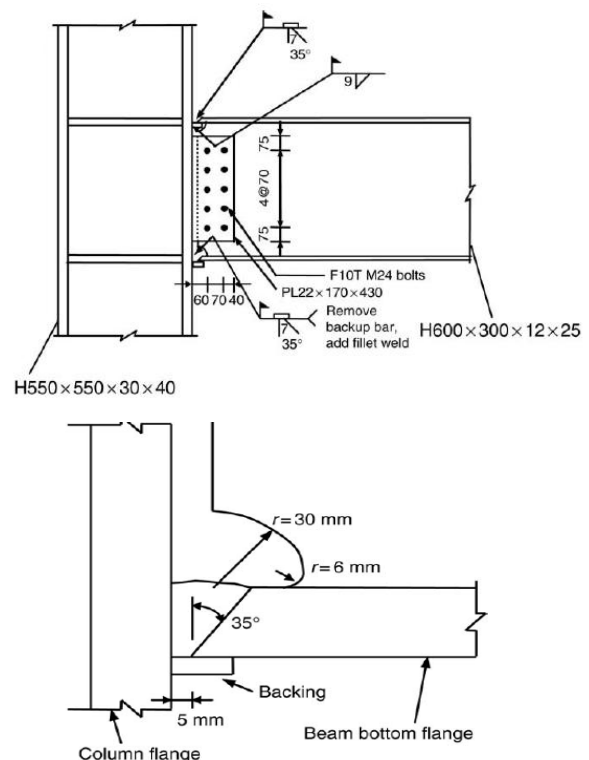


Fig.2. Connection geometry [11] of specimen S6

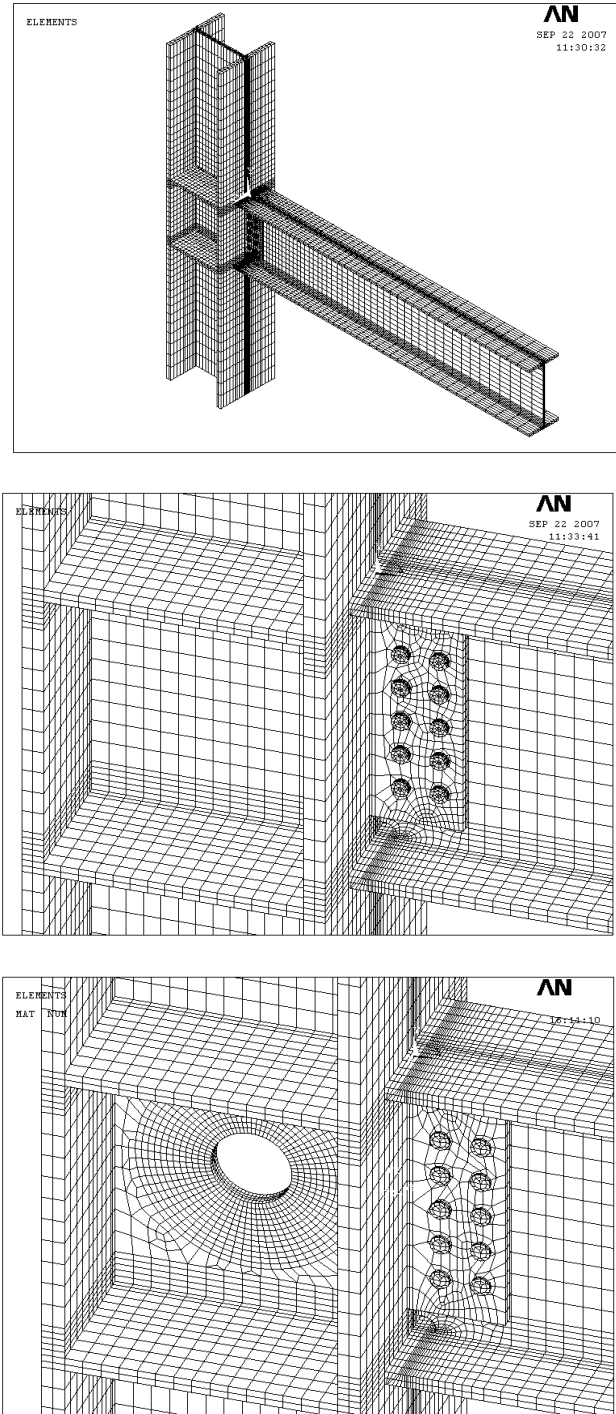


Fig.3. Finite element mesh for specimen S6 and specimen with a typical circular hole opening at the PZ

The balance ratio for specimen S6 is 0.7 and its total and PZ plastic rotations are 1.9 percent and 0.056 percent respectively. Since, the balance ratio is close to the lower bounds (0.6), it may be concluded that this specimen has strong PZ and that the contribution of the panel zone to the total plastic rotation of connection is very small. A circular hole was cut in the PZ area to increase the PZ plastic

rotation and consequently increase the balance ratio so that it will be close to the upper bounds (0.9). This would cause the PZ stiffness to decrease and its plastic rotation to increase.

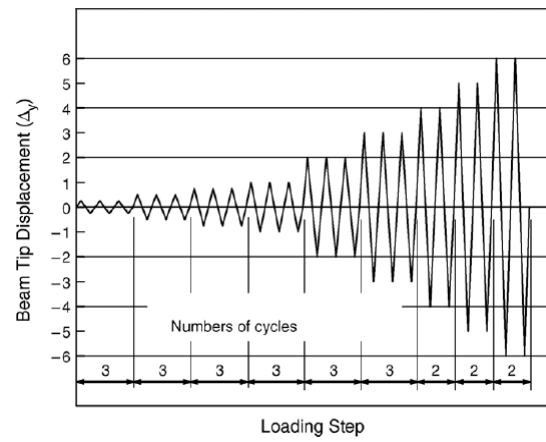


Fig.4. Displacement load history applied to the beam tip [11]

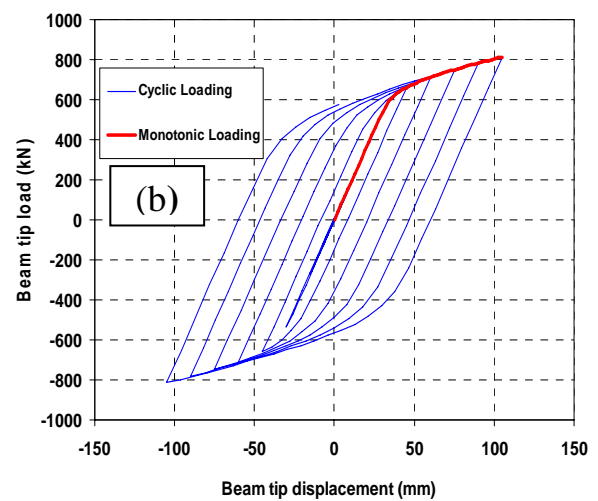
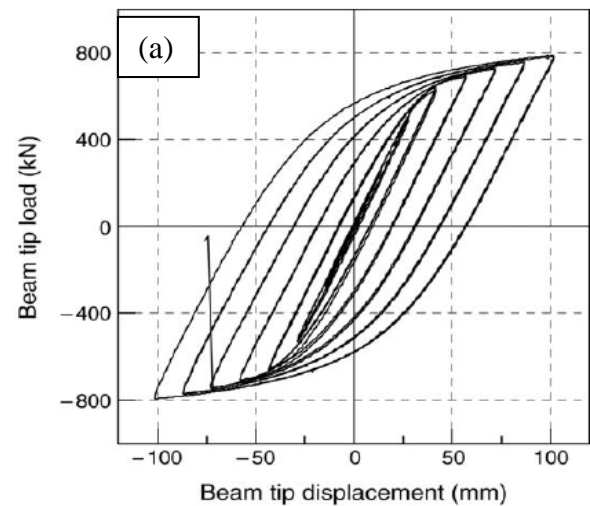


Fig.5. Experimental and analytical hysteresis curves for specimen S6: (a) experimental [11]; (b) finite element analysis.

It should be noted that excessive PZ rotation increases the stresses in beam flange and beam web (or shear tab) groove welds and consequently increases the fracture potential of connection. Therefore, a parametric study was needed to determine the optimum hole diameter to achieve the highest connection performance. Nine circular holes with different radiuses were considered in the PZ area (Fig.3).

The details of the circular holes and their balance ratios are tabulated in Table 1. This table shows that by increasing the PZ hole radius, R, the balance ratio also increases. This is due to the reduction in the PZ yielding resistance, V_y , which was calculated based on the elastic region of the PZ, using the PZ shear force versus PZ distortion curves. The end of each curve in Fig.6 indicates the failure of connection. Table 1 and Fig.6 show that by increasing the radius of the PZ hole, the stiffness of the PZ reduces, therefore, the total and the plastic PZ rotation also increases.

Post-Northridge connection failure was usually due to the fracture of the beam flanges at the access-hole region. In this study, the failure criterion was defined as the Von-Mises strains at whole beam flange widths at the weld access-hole region exceeding the strain associated with the ultimate strength of beam flange materials.

Equation 2 was obtained by introducing a reduction factor into Equation 1 and it can be used to determine the PZ yielding resistance, V_y , in the presence of a circular hole at PZ. The reduction factor is a polynomial, based on the ratio of hole diameter to PZ height, α ($\alpha=D/H$, where D and H are the hole diameter and clear PZ height respectively), and is obtained through a trial and error method. Fig.7 shows the results of the proposed PZ shear yielding resistance, equation 2, and actual yielding resistance obtained using finite element analyses. These are in good agreement.

$$V_y = Eq.1 \times [1 + \sum_{i=1}^5 (-\alpha)^i] \quad (2)$$

Fig.8 shows the total connection rotation versus normalized fracture moment curves, based on the beam plastic moment, for all specimens. Connection total rotation was calculated by dividing the beam tip deflection to the distance from the beam tip to the column web center and fracture moments were calculated at column face. As this figure shows, PZ

holes did not cause a remarkable reduction in normalized fracture moment even with the largest hole radius of 160 mm. The initial rotational stiffness of each connection was normalized with respect to the initial rotational stiffness of connection with no opening at PZ and is shown in Fig. 9. By increasing the hole PZ radius, R, the connection initial rotational stiffness reduced. However, for small value of R ($0 < R < 100$), the reduction in initial rotational stiffness was negligible.

Increase in the hole radius did cause a decrease in the total connection rotation. It is due to the increase in stresses (or strains) at critical locations (WAH root, CJP beam flange weld) caused by excessive panel zone distortion. Figs. 10.a and 10.b show normal strain distribution at specimens of an opening of 50 mm and 160 mm radius at PZ respectively. The spread of normal strains at bottom beam flange are higher for specimen of smaller void size (Fig. 10.a) when is compared with specimen of bigger void size (Fig. 10.b). However, the maximum normal strain at the most critical location, WAH root, of specimen of 160 mm void size was higher than smaller void size specimen (2 percent). These indicate firstly, the lower contribution of beam-end of specimen of 160 mm void radius and secondly higher possibility of fracture at specimen of 160 mm void size at WAH root.

Figs. 11.a and 11.b show shear strain distribution at specimens of an opening of 50 mm and 160 mm radius at PZ respectively. As these figures show and reported by other researchers, shear strains are at a minimum level at the center of the beam web, near the column face. However, shear stresses are maximum near the column flanges, especially at the most critical location, WAH regions (inverse of the classical beam theory). Comparison of Figs. 11.a and 11.b shows that by increasing the void radius from 50 mm to 160 mm, the maximum positive and negative shear strains increase 20 percent and 35 percent at WAH regions respectively. Combination of shear strains and normal strains at the beam flanges promotes the brittle fracture of welded connections. It is the reason of reduction of connection total rotation due to an excessive increase in PZ radius (Fig. 8).

Therefore, an increase in the plastic PZ rotation does not necessarily lead to an increase in total plastic rotation. Hence, the highest plastic rotation capacity is achieved with the optimum hole radius.

Table 1. Specimens with different PZ hole radiuses

No	PZ hole radius (mm)	V_y (KN)	$V_{PZ}^{(My)}$ (KN)	$V_{PZ}^{(Mp)}$ (KN)	$V_{PZ}^{(fail)}$ (KN)	$\frac{V_{PZ}^{(My)}}{V_y}$	$\frac{V_{PZ}^{(failure)}}{V_y}$	θ_{PZ}^{total} (%)	$\theta_{PZ}^{plastic}$ (%)	θ_{conn}^{total} (%)	$\theta_{conn}^{plastic}$ (%)	ψ
1	0	3400	2387	2657	3580	0.70	1.05	0.32	0.056	3.18	1.9	2.68
2	30	3110	2387	2657	3569	0.77	1.15	0.37	0.12	3.18	2.04	2.59
3	40	2983	2387	2657	3561	0.80	1.19	0.41	0.154	3.18	2.06	2.56
4	50	2935	2387	2657	3552	0.81	1.21	0.44	0.2	3.18	2.1	2.52
5	60	2827	2387	2657	3523	0.84	1.25	0.48	0.221	3.11	2	2.49
6	70	2743	2387	2657	3512	0.87	1.28	0.52	0.263	3.11	1.96	2.45
7	80	2691	2387	2657	3501	0.89	1.30	0.57	0.298	3.11	1.95	2.42
8	100	2547	2387	2657	3454	0.94	1.36	0.67	0.379	3.05	1.87	2.34
9	120	2410	2387	2657	3402	0.99	1.41	0.78	0.466	2.98	1.81	2.27
10	160	2144	2387	2657	3275	1.11	1.53	1.04	0.65	2.85	1.64	2.1

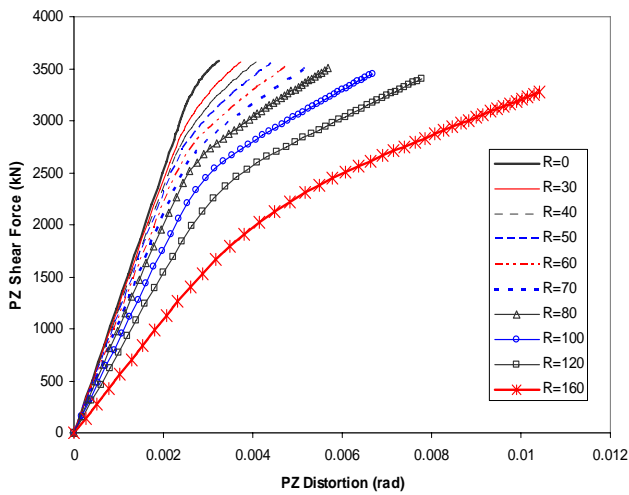


Fig.6. PZ shear force versus PZ distortion curves for different PZ hole radiuses

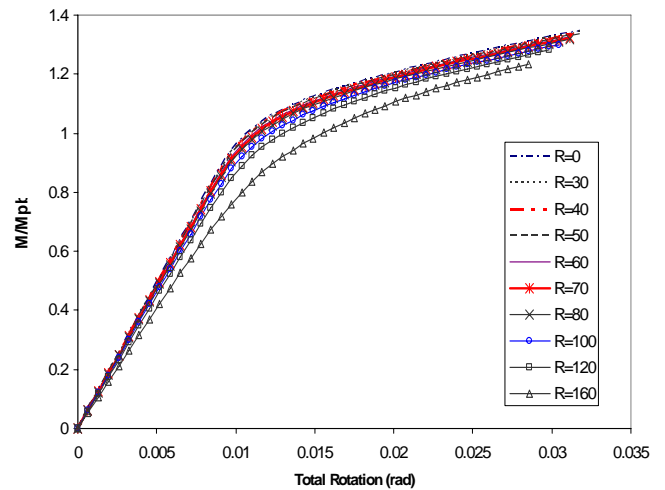


Fig.8. Total rotation versus normalized fracture moment for different PZ hole radiuses

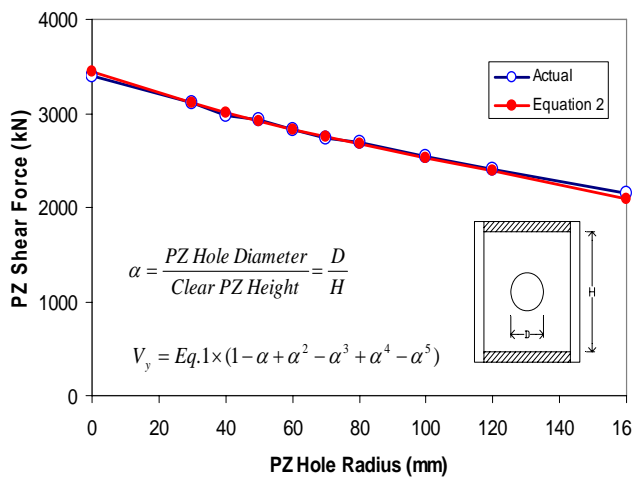


Fig.7. Comparison between the proposed and actual PZ yielding resistance

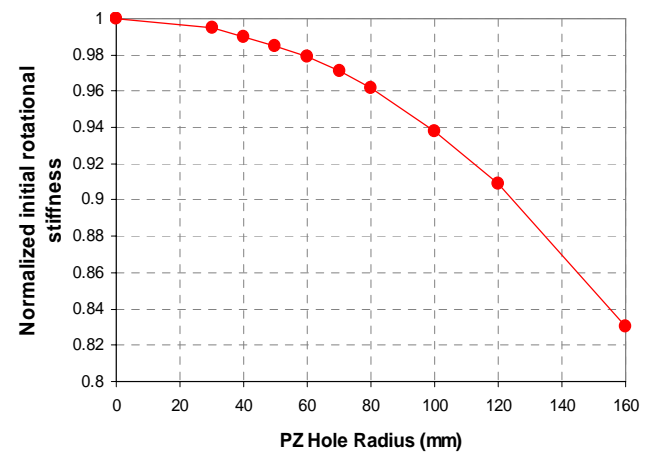


Fig.9. Normalized initial rotational stiffness for specimens of different PZ hole radiuses

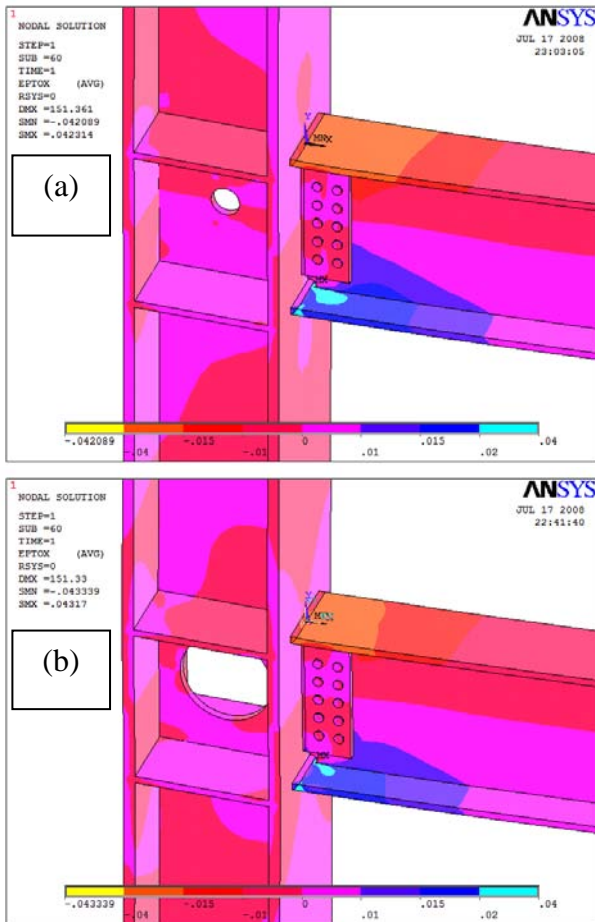


Fig.10. Normal strain distribution at specimens of a circular opening at PZ area of radiuses: (a) 50 mm; (b) 160 mm

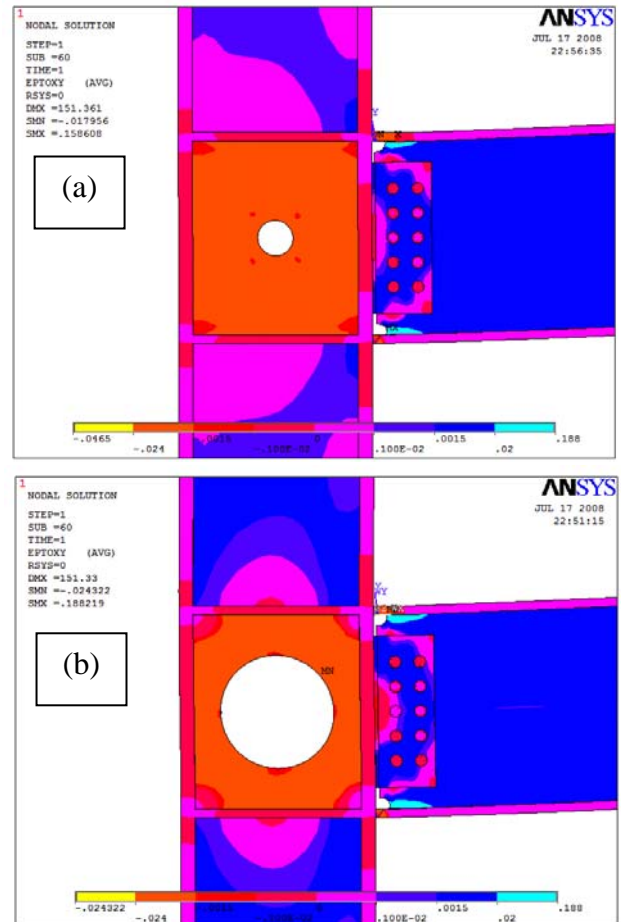


Fig.11. Shear strain distribution at specimens of a circular opening at PZ area of radiuses: (a) 50 mm; (b) 160 mm

Fig.12 shows the PZ plastic rotation versus the radius of the PZ hole. As the PZ hole radius increases from zero to 50 mm, there is an increase in both the connection and PZ plastic rotation. Despite the increase in the contribution of PZ to plastic rotation, the total plastic rotation decreases for PZ radius holes greater than 50 mm. This is due to the reduction of the contribution of the beam-end to plastic rotation.

It should be noted that opening a hole in the column web decreases the column plastic capacity. Since limited strain hardening occurs in post-Northridge welded flange-bolted web connections, then the probability of the occurrence of weak column bending failure mode increases. In order to control plastic deformation of columns and to ensure that the strong column-weak beam behavior is achieved, the limit ratio, which is defined in FEMA [6], should be greater than 1.1. This limit ratio is

$$\psi = \frac{\sum Z_c (f_{yc} - F / A_g)}{\sum Z_b \times f_{yb}} \quad (3)$$

where, Z_c , f_{yc} , F , A_g , Z_b and f_{yb} are column plastic section modulus, column yield stress, column axial force, column section area, beam plastic section modulus and beam yield stress. The limit ratios for all specimens are given in Table 1. Since these ratios are well over 1.1 the weak column bending failure mode will not occur.

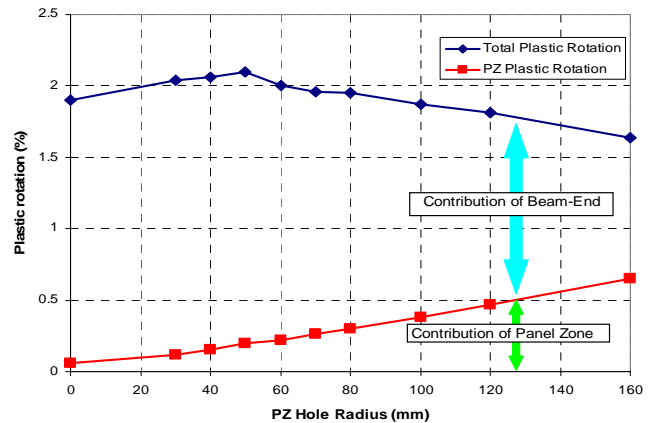


Fig.12 Contribution of PZ and End-Beam in total plastic rotation for different PZ hole radius openings

The results of finite element analyses are also presented in the form of PEEQ and rupture indexes. The PEEQ index is defined as the plastic equivalent strain (PEEQ) divided by the yield strain (ϵ_y) of the beam material (equation 4), which represents local strain demand. Rupture Index, RI, (equation 5) indicates the potential for fracture, such that, areas of connection with higher values of RI have a greater potential for fracture.

$$\text{PEEQ Index} = \sqrt{\frac{2}{3} \epsilon_{ij}^p \epsilon_{ij}^p} / \epsilon_y \quad (4)$$

$$\text{Rupture Index} = \frac{\epsilon_p / \epsilon_y}{\exp(-1.5 \frac{\sigma_m}{\sigma_{eff}})} \quad (5)$$

In these equations ϵ_{ij}^p , ϵ_p , ϵ_y , σ_m and σ_{eff} are plastic strain components, the equivalent plastic strain, yield strain, hydrostatic stress and Von-Mises stress respectively.

Figs. 13.a to 13.c show the PEEQ distribution at the WAH region for specimens of a circular opening of radius 0 mm, 50 mm and 160 mm at PZ area respectively. Increasing the void radius from zero to 50 mm, reduced the spread of PEEQ at WAH region and the maximum PEEQ reduced from 0.0946 to 0.092. However, excessive increase in void radius (160 mm) not only increased the spread of PEEQ at WAH region, but increased the maximum PEEQ up to 30 percent, from 0.092 to 0.1196 (compare Figs. 13.a and 13.c).

Figs.14 and 15 show the PEEQ index and rupture index for all specimens at four critical locations, WAH root, CJP welds at beam flange center, CJP welds at beam flange edge, and beam web welds or shear tab weld. Fig.14 shows that opening a circular hole of radius 60 mm in the PZ achieves the lowest level of the PEEQ index. Increasing the size of hole beyond 60 mm radius reduces the PEEQ index at WAH root and CJP welds at beam flange edge. On the other hand the PEEQ index increases for the CJP welds at the beam flange center.

Fig.15 shows that WAH root has the highest rupture index among all the critical locations, indicating higher potential for fracture at this point. This is clearly the reason for the initiation of fracture at this location in most of the pre and post-Northridge connection tests. Increasing the PZ hole radius reduces the rupture index at WAH root and CJP welds at the beam flange edge. However, for the CJP beam web and flange center, the rupture index starts to increase once the PZ hole radius exceeds 60

mm. Therefore, based on the achievement of maximum plastic rotation capacity of connection (Fig.12) and the results of the PEEQ and rupture indexes at critical locations (Fig.14 and Fig.15), it may be concluded that 50 mm is the optimum PZ hole radius, achieving a balance ratio of 0.81 and PZ hole ratio (α) of 18 percent.

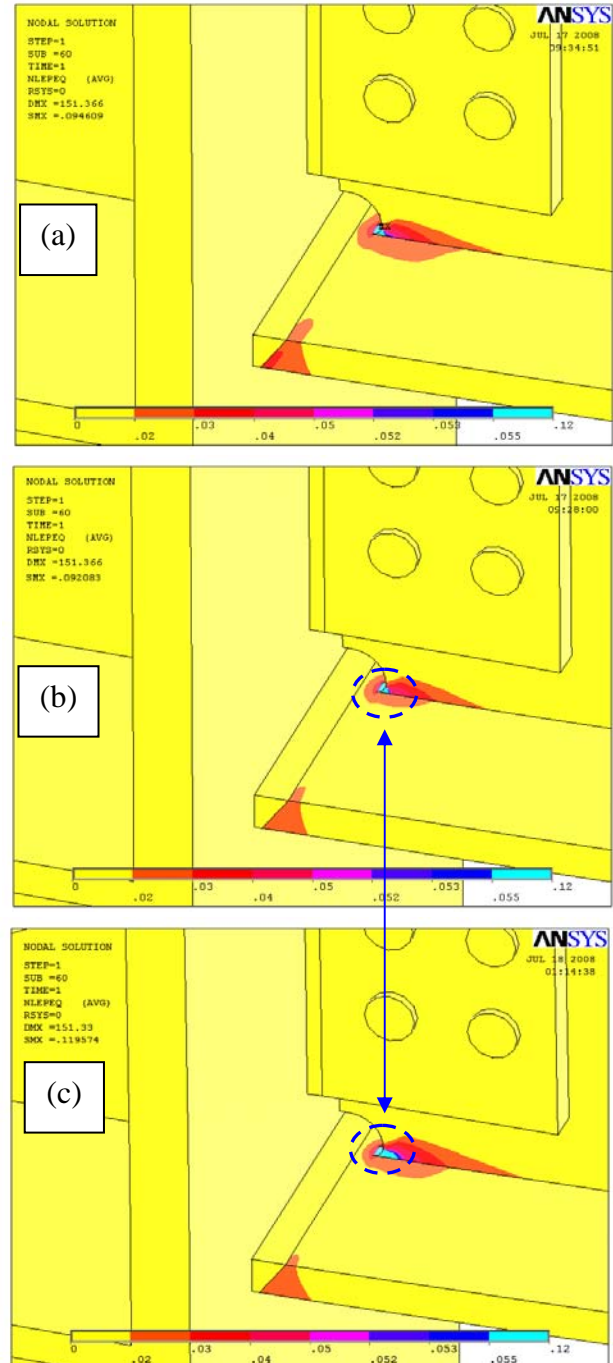


Fig. 13. Plastic equivalent strain (PEEQ) at the weld access hole region for specimens of a circular opening at PZ area of radiuses: (a) 0 mm; (b) 50 mm; (c) 160 mm.

By comparing Figs.13 and 14 a question might be raised that: Increasing the PZ void radius from 0 to 160 mm caused a 30 percent increase in the PEEQ at WAH region (Fig. 13), whilst such changes can not be seen in Fig. 14 at WAH root. The reason is as follow:

The WAH configuration of Specimen S6 (Fig. 2) was not exact accordance to the modified WAH configuration (Fig. 16, [16]), but there was still a small transition part (6 mm). Analytical results of reference [16] showed that the PEEQ, which is a measure of the local plastic strain demand, occurred at the toe of the weld access hole if the transition angle between the hole and beam flange was relatively sharp. This reference also showed that the maximum PEEQ moved up into the web along the weld access hole if there is a transition part.

In Fig. 14 PEEQ index was calculated at the root of WAH not at the transition part. These are the reason of having approximately constant PEEQ index at WAH root for specimens of different void size at PZ area.

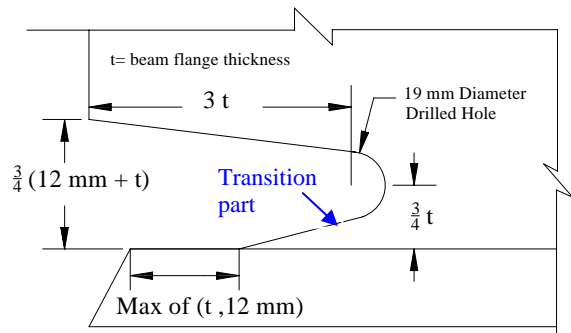


Fig. 16. Modified weld access hole geometry proposed in reference [16]

Although, a 50 mm circular hole caused a 300 percent increase in PZ plastic rotation, the total plastic rotation was only increased by 10 percent. The occurrence of early brittle fracture at these kinds of connections indicates that the connections also require modifications at the beam-end where more energy can be dissipated.

Finally, in order to illustrate the efficiency of the PZ holes on the development of the plasticization in the PZ area, plastic equivalent strains (PEEQ) are given in Figs.17 and 18 for specimens with a 50 mm PZ hole radius and without a PZ hole. These figures clearly show the difference between the spread of plastic strain at this source of dissipation of energy.

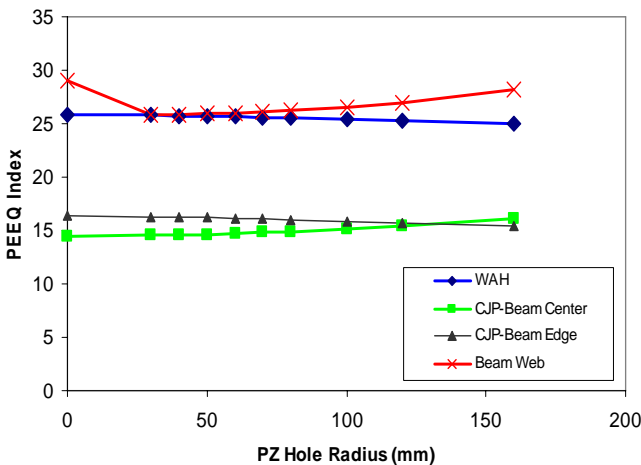


Fig.14. PEEQ index at critical locations for all specimens at 3% plastic rotation

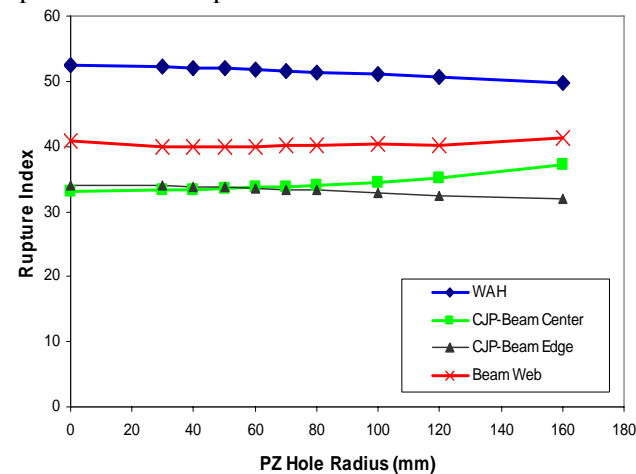


Fig.15. Rupture index at critical locations for all specimens at 3% plastic rotation

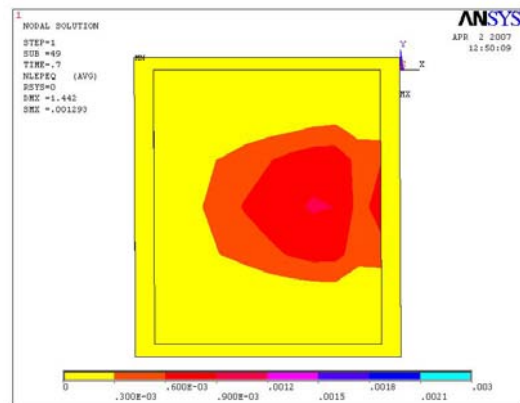


Fig.17. PZ PEEQ at failure, radius = 0 mm

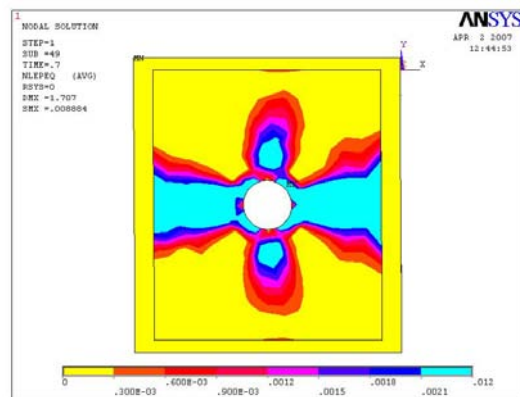


Fig.18. PZ PEEQ at failure, radius=50 mm

4 Conclusion

Various diameters of circular holes were made in the strong PZ area to achieve the FEMA balance condition for a strong PZ and consequently increase the contribution of strong PZ to the plastic rotation capacity of post-Northridge welded connection. These holes reduce the PZ rotational stiffness and consequently increase the PZ rotation. However, excessive PZ rotation increases the stresses at beam flange and beam web groove welds and consequently increases the fracture potential of connections. Therefore, a parametric study was conducted using finite element analyses to determine the most efficient hole radius that can achieve the highest connection plastic rotation capacity. Analytical results showed that among nine different sizes of circular holes, a PZ hole radius of 50 mm (with a PZ hole ratio of 18 percent) is the most effective for increasing the plastic rotation capacity of connection. At the same time, this 50 mm radius circular hole provided a reduction in PEEQ and rupture indexes at critical locations. This reduction was, however, more obvious for PEEQ index at beam web groove welds. Furthermore, the presence of a hole in the PZ, has only a small effect on the reduction of the total connection stiffness and normalized fracture moment, such that even for the largest PZ hole of 160 mm normalized fracture moment was greater than 1.2. Results also indicate that the circular hole at PZ will not lead to weak column bending failure mode (weak column-strong beam behavior).

Despite the increase in the PZ plastic rotation and total plastic rotation, the latter is still less than what is required for seismic regions (3 percent). Because of the occurrence of early brittle fracture in post-Northridge connections, this study also confirmed that there is a need to modify the configuration of the beam-end where more energy can be dissipated, which in return could also increase the contribution of the PZ to the plastic rotation capacity

References:

[1] Wang Xinwu, Experimental research and finite element analysis on Behaviour of Steel Frame with Semi-rigid Connections, *WSEAS Transaction on Heat and Mass Transfer*, Issue 3, Volume 2, July 2007.
[2] Chi W M, Deierlein G G, Ingraffea A R. Finite Element Fracture Mechanics Investigation of Welded Beam-Column Connections. *Report No. SAC/BD-97/05*, SAC Joint Venture 1997.
[3] Popov EP, Yang T, Chang S. Design of steel MRF connections before and after 1994 Northridge

earthquake. *Engineering Structures* 1998; 20(12): 1030–1038.

[4] S El-Tawil, T Mikesell, E Vidarsson, S K Kunnath. Strength and Ductility of FR Welded-Bolted Connections. *Report No. SAC/BD-98/01*, SAC Joint Venture 1998.

[5] Lee K H, Stojadinovic B, Goel S C, Margarian A G, Choi J, Wongkaew A, et al. Parametric Tests on Unreinforced Connections, *Report No. SAC/BD-00/01*, SAC Joint Venture 2000.

[6] FEMA, State of the art report on connection performance. *Report No. FEMA 355D*, Washington, September 2000.

[7] Lu L, Ricles J, Mao C, Fisher J. Critical issues in achieving ductile behavior of welded moment connections. *Constructional Steel Research*, 2000; 55: 325-341

[8] Ricles JM, Fisher JW, Lu L-W, Kaufmann EJ. Development of improved welded moment connections for earthquake-resistant design. *Journal of Constructional Steel Research*, 2002; 58:565–604.

[9] L. Vasiliauskiene, S. Valentinavicius, A. Sapalas, Adaptive Finite Element Analysis for Solution of Complex Engineering Problems, *WSEAS Transactions on Applied and Theoretical Mechanics*, Vol.1, No.1, 2006.

[10] Z.L. Mahri, M.S, Rouabah, Calculation of Dynamic Stresses using Finite Element Method and Prediction of Fatigue Failure for Wind Turbine Rotor, *WSEAS Transactions on Applied and Theoretical Mechanics*, Issue 1, Volume 3, January 2008.

[11] Chen CC, Chen SW, Chung MD, Lin MC. Cyclic behavior of unreinforced and rib-reinforced moment connections. *Journal of Constructional Steel Research*, 2005; 61(1):1–21.

[12] ANSYS User Manual. ANSYS, Inc., 2007.

[13] Bahaari M.R, Sherbourne A.N. Behavior of eight bolt large capacity endplate connections. *Computers and Structures*, 2000; 77: 315-325

[14] Coelho A.M, Bijlaard F, Nol Gresnigt N, Da Silva LS. Experimental assessment of the behaviour of bolted T-stub connections made up of welded plates. *Journal of Constructional Steel Research*, 2004; 60: 269–311

[15] Bursi O.S, Jaspert J.P. Basic issues in the finite element simulation of extended end plate connections. *Computers and Structures*, 1998; 69: 361-382.

[16] Lu L, Ricles J, Mao C, Fisher J. Critical issues in achieving ductile behavior of welded moment connections. *Journal of Constructional Steel Research* 2000; 55: 325-341.